This is an open access article published under a Creative Commons Attribution (CC-BY) License, which permits unrestricted use, distribution and reproduction in any medium, provided the author and source are cited.

ACS AUTHORCHOICE Article

THE JOURNAL OF PHYSICAL CHEMISTRY A

pubs.acs.org/JPCA

Forming NCO^- in Dense Molecular Clouds: Possible Gas-Phase Chemical Paths From Quantum Calculations

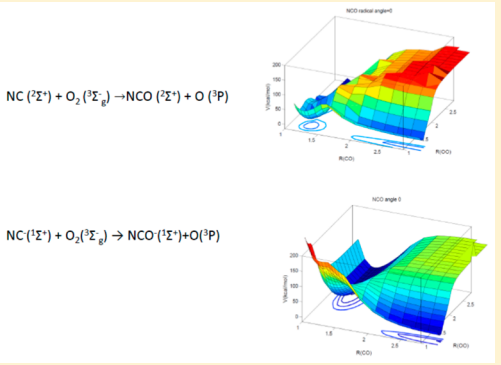
E. Yurtsever,[†] F. A. Gianturco,*[,‡,§] and R. Wester[‡]

[†]Department of Chemistry, Koç University, Rumelifeneriyolu, Sariyer, TR-34450, Istanbul Turkey

[‡]Institut für Ionen Physik und Angewandte Physik, Leopold-Franzens-Universität, Technikerstraße 25, 6020, Innsbruck, Austria

[§]Scuola Normale Superiore, Piazza Cavalieri 7, 56126 Pisa, Italy

ABSTRACT: The existence of NCO^- anions in the interstellar medium (ISM) has been suggested and searched for over the years but without any formal definitive sighting of that molecule. We discuss in this work the possible formation of either NCO^- directly or of NCO neutral as a precursor to NCO^- formation by electron attachment. We follow simple, gas-phase chemical reactions for which the general features are obtained from accurate quantum calculations. The results are shedding some additional light on the likely presence of this anion in the ISM environment, drawing further information from the specific features of the considered reactions on the additional chemical options that exist for its formation.



1. INTRODUCTION

The presence and role of molecules carrying a charge has been recognized for a long time as playing a significant role in the gas-phase chemistry of the interstellar space.[1,2] The existing chemicals, and especially H and H_2, are in fact ionized in the diffuse regions of the interstellar medium (ISM) by cosmic rays and can produce both ionic species and free electrons, which can in turn recombine with the neutrals present to further form anionic molecules. The starting of several ion−molecule reactions therefore yields a broad variety of species in the outer regions of the diffuse molecular clouds,[3] where many of them have been observed.

The situation in the colder dark molecular clouds (DMC) is however different because the presence of the more penetrating electrons from the outer regions still exists whereas there is a corresponding partial blocking of the photon flows from external sources. Such penetrating electrons can in turn activate chemical processes where e^- plays an important role informing novel anionic partners. Earlier estimation of the relative abundances of free electrons in the dark clouds indicate it to be about 4×10^{-8} with respect to H_2[4] which is comparable or larger than that of most neutral molecules observed in these clouds.

Given the existence of many simple molecules with large, positive electron affinities (EA), it is also possible that negatively charged molecular species can exist there and would survive due to the reduced influence of photodetachment channels. It was pointed out a while ago[5] that those negative ions if formed would rapidly undergo electron loss by photodetachment processes induced by the cosmic radiation while the inner cores of the dark molecular clouds would be partially shielded from the outer photon sources and therefore "protect" the anions from photodetachment.

The earliest discovery of a molecular anion in the ISM has occurred in the experiments of McCarthy et al.[6] It was followed by the observation of the carbon chains of the type $C_{2n}H^-$ and $C_{2n+1}N^-$ by Cernicharo's group.[7] They were found in the circumstellar envelope of a source labeled IRC+10210 and in other dark clouds like TMC1. The negative ion CN^- has also been observed in DMCs, where its neutral counterpart, CN, was also detected by the same group.[8]

Since those findings, therefore, the possibility of molecular anions existing within the colder DMCs has become an item of research in molecular astrophysics, and possible chemical routes that involve change−exchange in ion−molecule reactions have been investigated in the case of $C_{2n+1}N^-$ formation paths, just to give an example from our own work[9] in this area.

The present study therefore intends to present a computational analysis of ion−molecule reactions that could lead to the formation of yet another molecular anion, the NCO^-, a stable species exhibiting a closed-shell $^1\Sigma^+$ ground electronic state, a large positive electron-affinity of 3.609 eV[10] and a permanent dipole moment of 1.5 D,[11] which is not far from what is called a "critical" value of ∼1.67 D.[9] The meaning of this comment will become clearer in the discussions of Section 3.

Special Issue: Piergiorgio Casavecchia and Antonio Lagana Festschrift

Received: October 26, 2015
Revised: December 14, 2015
Published: December 22, 2015

ACS Publications © 2015 American Chemical Society

DOI: 10.1021/acs.jpca.5b10472
J. Phys. Chem. A 2016, 120, 4693−4701

Downloaded from pubs.acs.org/jpcafh/article-pdf/120/27/4693/6721384/acs.jpca.5b10472.pdf by KOC UNIV user on 25 October 2026

Its rotational constants have been observed in the laboratory using a supersonic molecular beam experiment[12] and a tentative assignment of the absorption band at 2157 cm^{-1} to the NCO^- anion was put forward in a few recent papers,[13,14] where it was suggested that this anion originated from acid−base reactions on interstellar grains. Further, more quantitative studies from laboratory experiments surmised the formation of NCO^- in DMCs from ice-supported reactions that would involve a variety of cyano-derivatives and water,[15] thus paving the way to the further possible presence of its anion.

Direct observations of several simple molecular anions, including NCO^-, were carried out recently[16] by extensively searching in the DMC L134N, using the Nobeyama 45 m radio telescope. Additional searches were also performed in the translucent cloud CB228 and in the star-forming region in Sagittarius, SgrB2. The authors[16] concluded that their upper limit to the column density for NCO^- was obtained to be 1×10^{12}, which corresponds to a fractional abundance of NCO^- of 5×10^{-11} relative to H_2. This finding suggests small abundances that, however, do not yet allow for a clear identification of this anion.

One of the most direct and often suggested paths to anion formation in DMCs is the radiative electron attachment (REA) process

$$NCO + e^- \rightarrow NCO^- + h\nu \quad (1)$$

The corresponding rate at low temperatures is not yet known for this system, although the corresponding elastic scattering of low-energy electrons has been obtained from R-matrix calculations[17] and, as expected, has been found to yield very large cross sections at low energies. Direct calculations of the REA rates for CN^- formation have, however, found them to be very small at around 10 K,[18] about 10^{-15} cm^3/s, indicating that the competing process of autodetachment is the dominant decaying route for dissipating the excess energy after temporary attachment[18] in the cases of small (2−3 atoms) molecular species. Hence, given the size and chemical similarity between these molecules, the same might occur for the NCO^- as we shall further discuss below.

Another often suggested option for the NCO^- formation has been given by the chemical reaction routes involving oxygen molecules and the (observed) cyanide radical or the cyanide anion itself.[12] In the present study, we shall therefore analyze the energy landscapes for two possible reactions involving oxygen molecules, which are present in DMC environments, and either the CN^- anion or its neutral counterpart (their specific electronic states will be further discussed later)

$$CN^- + O_2 \rightarrow NCO^- + O \quad (2)$$

$$CN + O_2 \rightarrow NCO + O \quad (3)$$

We shall demonstrate in the following that both reactions are strongly exothermic processes so that the possibility might exist for them to take part into the formation of NCO^-, either directly via eq 2 or indirectly via eq 3, followed by the REA process of eq 1.

2. THE AB INITIO STRUCTURAL ENERGIES

As mentioned in the Introduction, we intend to carry out accurate quantum chemical calculations regarding the energetics and the potential energy landscapes of the possible chemical routes involving CN and O_2, both in the radical and ionic reactions, that is, involving either CN or CN^-: both such species have been, in fact, already observed, and therefore exist in the ISM environments so that it makes physical sense to further investigate their role in the chemistry of NCO^- formation.

All calculations were carried out using the Gaussian09 quantum chemistry software[19] and the specific details of the various runs will be discussed in each sub sections below. In both sets of calculations, we have employed the MP2 approach, using the aug-cc-pV5Z expansion to describe the two reacting molecules.

a. The Radical Reaction. The reaction which we shall discuss below involves the following partners

$$NC(^2\Sigma^+) + O_2(^3\Sigma^-_g) \rightarrow NCO(^2\Sigma^+) + O(^3P) \quad (4)$$

The reagents' geometries were optimized at the beginning of the calculations, yielding the final values reported in Table 1.

Table 1. Computed Energy Gap Values for the Radical Reaction 4[a]

method	ΔE (kcal/mol)	ΔE^* (kcal/mol), ZPE corrected
MP2/aug-cc-pVTZ	−25.39	−24.51
MP2/aug-cc-pVQZ	−24.65	−23.82
MP2/aug-cc-pV5Z	−24.51	−23.97
CCSD(T) /aug-cc-pVTZ	−21.47	−20.94
CCSD(T) /aug-cc-pVqZ	−20.32	−19.77
CCSD(T) /aug-cc-pV5Z	−19.99	−19.44
CBS	−19.58	−19.00

[a]See text for further details.

The product NCO at its equilibrium geometry was also obtained with the same level of calculations as reported in that table. All values are in very good accord with recent calculations on the same system,[20] so we can consider the above parameters to be quite accurate in describing the reacting species.

Another interesting set of values that will help us to further assess the feasibility of this radical reaction is the evaluation of the energy difference between reagents and products. We then calculated the exothermicity of the reaction also using the MOLPRO suite of programs.[21,22] The reagents and products where described at their optimized geometries resuming the complete basis set (CBS) limit. The MP2 and CCSD(T) descriptions of the wave function using aug-cc-pVXZ with X = T, Q, and 5 was also employed in order to follow the quality of the results as the basis set expansion was varied. Our findings are reported in Table 1.

The table values are given as negative numbers meaning that the radical reaction is a strongly exothermic reaction with an energy gain which is around 0.8 eV from reactants to products. We also see that increasing the size of the basis set and reaching the CBS limit (bottom line) reduces gradually the exothermicity, converging to a value close to 20 kcal/mol, which is fairly substantial for a reaction in the ISM environment. Furthermore, when the zero-point-energy (ZPE) correction is added to both asymptotic configurations the gap is slightly further reduced, as can be seen from the data marked by asterisk in the third column in the table. Thus, we can say that our best result for the reaction's exothermicity is around 19 kcal/mol.

The corresponding trend of the optimized molecular configurations, as a function of the basis set size, is further reported by the data shown in Table 2.

Downloaded from pubs.acs.org/jpcafh/article-pdf/120/27/4693/6721384/acs.jpca.5b10472.pdf by KOC UNIV user on 25 October 2026

DOI: 10.1021/acs.jpca.5b10472
J. Phys. Chem. A 2016, 120, 4693−4701

Table 2. Geometrical Parameters of the Reactants and Products from MP2 Optimizations[a]

	aug-cc-pVTZ	aug-cc-pVQZ	aug-cc-pV5z
R(N−C) in NC	1.126	1.123	1.122
R(O−O) in O_2	1.224	1.219	1.218
R(N−C) in NCO	1.248	1.245	1.244
R(C−O) in NCO	1.158	1.155	1.154

[a]All values are in units of angstroms.

We have further searched for the presence of a transition state (TS) using the largest basis set at the MP2 level and mapping the entire surface over more than 1000 points. We were not able to locate a proper TS, thereby coming to the conclusion that this radical reaction is markedly exothermic and it proceeds from reagents to products without a barrier, hence not forming a transition state. To further clarify this last point, we show in Figure 1 the overall behavior of the lowest

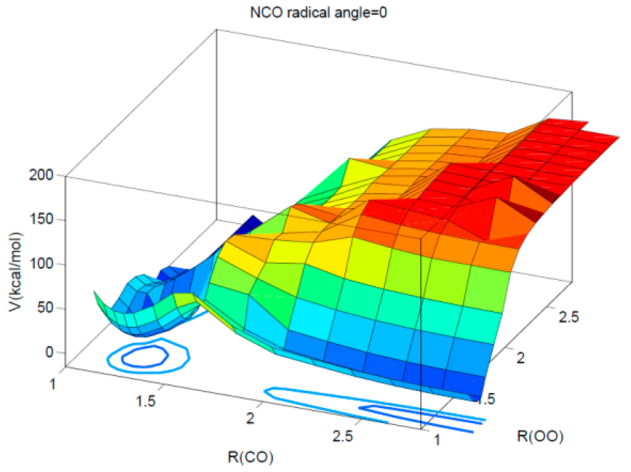


Figure 1. Computed reactive PES for the radical reaction of eq 4. See main text for further comments. Distances are in angstroms.

electronic potential energy surface (PES) as a function of two relative distances: R_{CO}, the distance between the C atom of CN and the nearer O atom of O_2, and R_{OO}, the relative distance between two oxygen atoms. The orientation angle Θ describes the bending of one R_{CO} distance with respect to the R_{OO} distance. In the actual figure we report, as an example, the case for the collinear approach between reagents at the C-side (Θ = 0). The CN distance is kept at its equilibrium value of 1.12 Å and does not change much in the final NCO molecule (see Table 2).

The observed exothermic reactivity along the reaction path is clearly displayed by the features of that energy map: on the "upper" far left we see the stable formation of NCO, while on the near upper right one recognizes, starting around the equilibrium bond of O_2 (about 1.218 Å), the evolution of a minimum energy path (MEP) that involves at first a " vibrationally cold" oxygen molecule and that presents a barrier along its way to the reagents' complex on the lower left side of the map. On the other hand, as the O_2 bond is stretched we see more clearly a steady decrease of the interaction energy from reagents to products without any barrier; this reaction, therefore, occurs upon O−O dissociation during the interaction of the initial O_2 partner with the approaching CN. These features will be further discussed below in additional figures.

It is also interesting to note here that the radical reaction, when looking at different orientations of the angle Θ between the NC and O−O bonds, appears to be largely proceeding via an uphill MEP whenever the oxygen molecular partner remains vibrationally cold and is not stretched out to near dissociation. A specific example of these data is shown by Figure 2, where we have chosen Θ = 90° approach to describe its behavior.

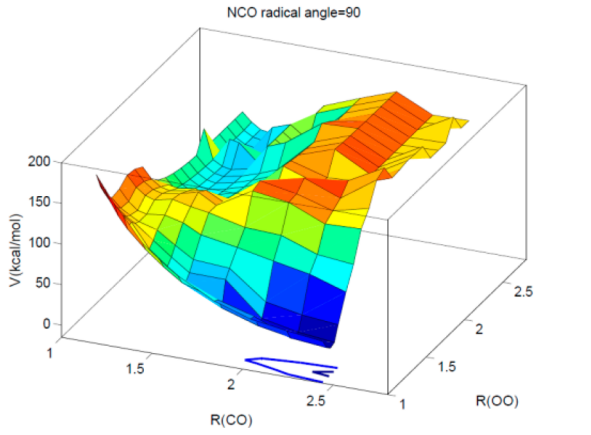


Figure 2. Similar data to those of Figure 1 but for the different orientation angle Θ = 90°. The units are the same as in Figure 1. See main text for a more extended discussion.

It is clear from that figure (where lack of smoothness is due to numerical noise) that for the stretched O−O distances, that is, for geometries away from the R_{OO} equilibrium structure, the surface remains always without barrier and exothermic toward the left region of the NCO product. However, if that distance were to be kept artificially fixed at the O_2 equilibrium value, a barrier would appear. We think that the forcing of the oxygen bond to remain rigidly at its equilibrium value during the reactive approach is really unphysical for the present reaction since it disregards the fuller action of chemical forces while the partners approach each other.

This point is further graphically presented by the data of Figure 3, which now reports different "cuts" of the reactive

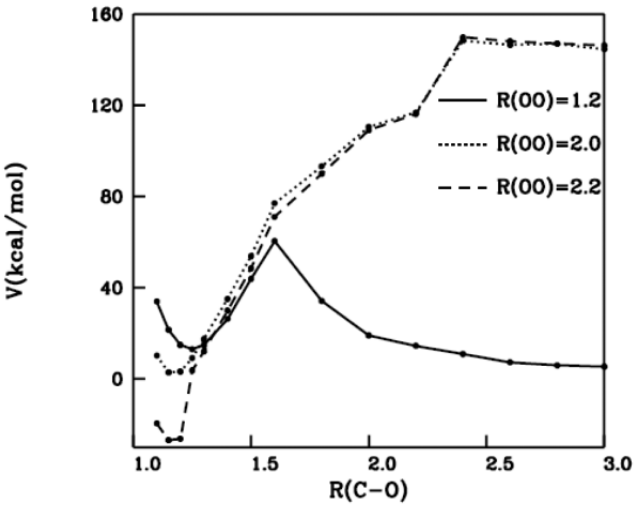


Figure 3. Reactive PES behavior along the NC···OO distance and for different values of the R_{O-O} bond length. See main text for additional comments.

Downloaded from pubs.acs.org/jpcafh/article-pdf/120/27/4693/6721384/acs.jpca.5b10472.pdf by KOC UNIV user on 25 October 2026

DOI: 10.1021/acs.jpca.5b10472
J. Phys. Chem. A 2016, 120, 4693−4701

surface described in Figure 1. These specific curves are taken for fixed CN bonds at the equilibrium value but selecting three different oxygen bond values and plotting the energy behavior as the CO distance is changed.

If one considers in that figure the O_2 reacting partner coming in toward the NC molecule (going from right to left along the "cuts") we see that when the O_2 bond stretches during the approach to the reaction region, then the reaction remains barrier-less and clearly exothermic. If one however forces the O_2 molecule to remain close to its equilibrium geometry (∼1.2 Å) during the approach, this constraint induces the appearance of a barrier, which is however canceled as the full reaction occurs and one of the oxygen atoms departs from the complex while approaching the CN partner.

This situation becomes even more apparent if we generate the cuts for fixed R_{CN} and R_{CO} distances but as a function of the R_{OO} distance, as shown by the plot of Figure 4.

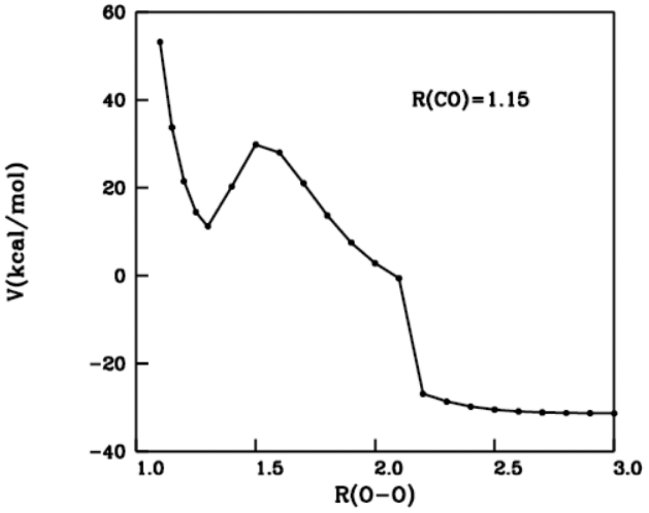


Figure 4. Computed energy cut for the reactive PES along the R_{OO} distance, while the R_{CN} and R_{CO} are kept fixed. See main text for additional discussion.

The above figure shows a marked barrier when the O_2 molecule is forced to remain close to its equilibrium value. On the other hand, when that bond distance is allowed to stretch, that is, one of the oxygen atoms is allowed to move away as the reaction progresses, we now see that the process of forming NCO becomes clearly exothermic and without an energy barrier. This indicates that a description of the energy landscape for the full reactive PES should involve all three chemical bonds: it will then be describing a radical reaction that does not present a barrier to product formation and that occurs concurrently as the partner O_2 moves to its dissociation during the reactive approach. In fact, when we have optimized the total wave function for all geometries at each grid-point, the barrier seen in Figures 3 and 4 entirely disappear, as expected from the analysis above.

When we further analyze the behavior of the local charge distributions in the barrier region, we find that at about 1.7 Å of the distance between NC and OO partners, and keeping the other two distances close to their equilibrium values as in Figures 3 and 4, now indeed a major charge rearrangement occurs: the NC fragment behaves as a cationic partner with a positive partial charge of 0.4 at the distances smaller than 1.7 Å, while after that value a charge-migration occurs and an anionic NC with a relative charge of −0.4 is formed. This generates a sort of "bond dilution" for the oxygen's molecular bond during the reactive approach. It thus indicates that the exothermicity of the reaction along the MEP is justified by this concurrent stretching effect as the product molecule is formed. One can therefore argue that the present calculations for the reactive path show this radical reaction to be without a barrier to product formation, and also is exothermic, as long as the O_2 molecular partner helps to stabilize the final NCO product via its concurrent bond stretching. Additionally, no other electronic states were found here to be coming close enough during the present reactive evolution on the lowest electronic configuration to be playing a significant role in it.

A full summary of the numerical results that we have obtained for the radical reaction is collected in Table 3, where

Table 3. A Summary of the Computed Energetics (MP2 Calculations) for the Radical Reaction 4[a]

	Total Energy (au)		
species	aug-cc-pVDZ	aug-cc-pVTZ	aug-cc-pVQZ
NC	−92.451672	−92.521340	−92.544873
O_2	−150.004290	−150.120938	−150.160430
NCO	−167.591514	−167.723440	−167.767876
O	−74.906967	−74.959294	−74.976709
	Thermochemical Gap (kcal/mol)		
	aug-cc-pVDZ	aug-cc-pVTZ	aug-cc-pVQZ
without ZPE	−26.68	−25.39	−24.65
with ZPE	−25.70	−24.51	−23.82

[a]See main text for further details.

we clearly see the strong exothermicity and the lack of a barrier to a transition state structure. This reaction should therefore be a strong candidate for NCO formation at the low temperatures of the dark molecular clouds because our calculations detect no energetic hindrance for the reacting partners to reach the products' region. The chemical formation of the neutral radical would then be the first step to the final anion formation via reaction 1, as we shall further discuss below.

B. The Ion–Molecule Reaction. As mentioned earlier, the other option for the direct formation of the NCO^- anion via chemical reaction with oxygen molecules would be a reaction between neutral oxygen and the CN^- species

$$NC^-(^1\Sigma^+) + O_2(^3\Sigma^-_g) \rightarrow NCO^-(^1\Sigma^+) + O(^3P) \quad (5)$$

As before, we have optimized the geometries of both reagents and products by using again the Gaussian09 suite of codes at the MP2 level and employing an expansion at the aug-cc-pV5Z level. All the present values agree well with those reported by Leonard et al.[20] The computed trend of geometric changes with the basis set expansions is reported by Table 4.

Table 4. Dependence of Bond Values on Basis Set Choices[a]

	aug-cc-pVTZ	aug-cc-pVQZ	aug-cc-pV5z
R(N–C) in NC^-	1.191	1.187	1.187
R(O–O) in O_2	1.224	1.219	1.218
R(N–C) in NCO^-	1.204	1.201	1.200
R(C–O) in NCO^-	1.233	1.230	1.229

[a]All values are in angstroms.

Downloaded from pubs.acs.org/jpcafh/article-pdf/120/27/4693/6721384/acs.jpca.5b10472.pdf by KOC UNIV user on 25 October 2026

DOI: 10.1021/acs.jpca.5b10472
J. Phys. Chem. A 2016, 120, 4693–4701

We further computed the thermochemistry of the reaction using the MOLPRO suite of codes[21,22] at the complete basis set limit (CBS) and also compared the changes when using different basis set expansions. The results are reported in Table 5 and clearly show that also this ion−molecule reaction is markedly exothermic with an energy gain of about 0.46 eV. To our knowledge, no data on this reaction had been obtained previously to the present study.

Table 5. Computed Energy Gap (ΔE) of the Ionic Reaction[a]

method	ΔE (kcal/mol)	ΔE* (kcal/mol), ZPE corrected
MP2/aug-cc-pVTZ	−10.77	−9.14
MP2/aug-cc-pVQZ	−10.40	−8.79
MP2/aug-cc-pV5Z	−10.36	−9.02
CCSD(T) /aug-cc-pVTZ	−11.43	−9.96
CCSD(T) /aug-cc-pVqZ	−11.04	−9.54
CCSD(T) /aug-cc-pV5Z	−10.93	−9.41
CBS	−10.78	−9.25

[a]See main text for details. The data in the third column are obtained by also including the ZPE corrections.

The results reported in that table are all given in kcal/mol and follow the expected trend. The data of the third column include ZPE corrections and again indicate a small, but constant reduction effect on the final thermochemical exothermicity of this reaction.

As in the previous case, we have analyzed the landscape of the reactive PES in its lowest electronic state to identify the possible presence of a transition state configuration and also the possible barrier along the MEP to products. This feature turned out to be absent for the case of the radical reaction, which we have discussed in the previous subsection.

We searched for a possible TS state by looking for a single negative eigenvalue of the Hessian for a series of different basis set expansions, as reported at Table 6. Given the good internal consistency of the results, we believe that our more extended calculations at the aug-cc-pVQZ level are accurately predicting in this case the presence of a transition state [NCOO$^-$] in a linear geometry (Θ = 0°).

Table 6. Computed Geometry and Energy Parameters for the Linear Transition State of the Ion−Molecule Reaction as a Function of the Level of Calculations[a]

	MP2/aug-cc-pVDZ	MP2/aug-cc-pVTZ	MP2/aug-cc-pVQZ
R(NC)	1.188	1.175	1.172
R(CO)	1.747	1.733	1.730
R(OO)	1.577	1.569	1.566
activ.E.	99.4	101.0	102.2
act.E. ZPE corr.	99.8	102.9	104.0
reaction energy	−10.87	−10.77	−10.40
backward activ.E.	110.3	111.9	122.6
backward act.E. ZPE corr.	110.9	112.1	112.8

[a]All data are in either angstroms or kcal/mol.

The results in Table 6 clearly indicate the presence of an energy barrier when going from the reactants to products along the collinear path. An accurate, graphical description of the existing barrier along that path is given by carrying out intrinsic reaction coordinate (IRC) calculation. The latter quantity has been defined long ago in the literature[23] and also more formally linked to the Hamilton-Jacobi theory.[24] Qualitatively speaking, it represents the mass-weighted coordinate representation of the steepest-descent curve along the reaction path to either reagents or to products from the transition state location.

The results from the present analysis are given in Figure 5.

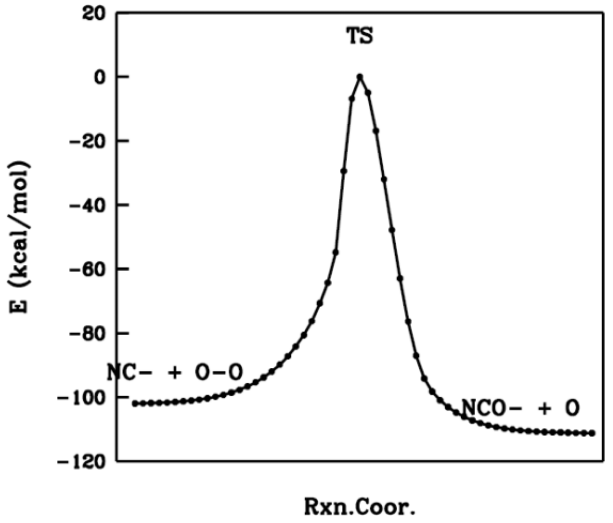


Figure 5. Energy profile of the transition state location along the IRC representation of the ionic reaction 5. See main text for additional discussion.

One sees from the data of Table 6 that the collinear approaches produce the most stable MEP for the complex, as confirmed by the IRS profile of the Figure 5, where a collinear configuration exists for the transition state (TS) geometry. It means that the physical occurrence of the energy lowering along the path takes place as one oxygen atom moves away from the complex and the reaction occurs along that path. A further verification for the presence of a TS configuration on top of a barrier could be had by repeating the calculations along the same R_{CO} coordinate of Figure 4 but now by optimizing the bond lengths in NC and O_2; it will help us to go from reagents to products along the collinear path outlined in Figure 5. The results are given in Figure 6.

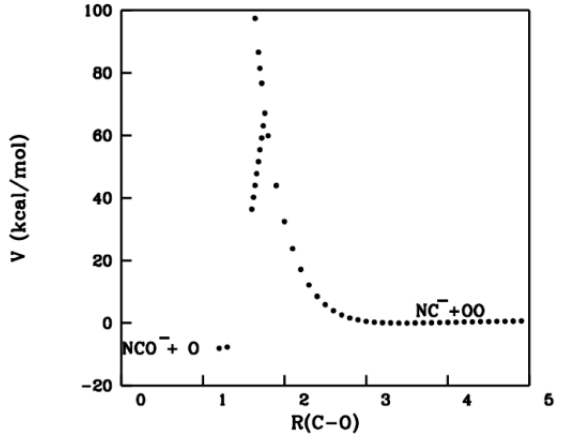


Figure 6. Computed energy profiles, as a function of the R_{CO} distance between CN^- and OO, by optimizing the two molecular distances at each step. Distances in angstroms.

DOI: 10.1021/acs.jpca.5b10472
J. Phys. Chem. A 2016, 120, 4693−4701

Downloaded from pubs.acs.org/jpcafh/article-pdf/120/27/4693/6721384/acs.jpca.5b10472.pdf by KOC UNIV user on 25 October 2026

These calculations for the energy profiles confirm the occurrence of a special configuration (the TS geometry) for which the relative energy presents a barrier, as already indicated in Figure 5.

By moving at different angles, we can further obtain additional information and thus extract the thermochemical behavior as a function of the bending angle between two reagents, NC^- and O_2. Thus, the energy gap can be obtained now from the NCO^-+O energy with reference to that of the two reactants kept at a fixed angle in the reactive regions of the TS. The results are summarized by Table 7.

Table 7. Computed Thermochemical Energy Gaps as a Function of the Orientation between Initial Reagents[a]

Θ	Δ *E*(kcal/mol)
0°	−12.64
15°	−9.56
30°	1.10
45°	40.14
60°	70.15
75°	104.04
90°	130.09

[a]The Θ = 0° corresponds to the $[NCO\cdots O]^-$ structure.

We additionally present in Figure 7 the energy profiles obtained by freezing the CN distance at 1.207 Å and the O−O

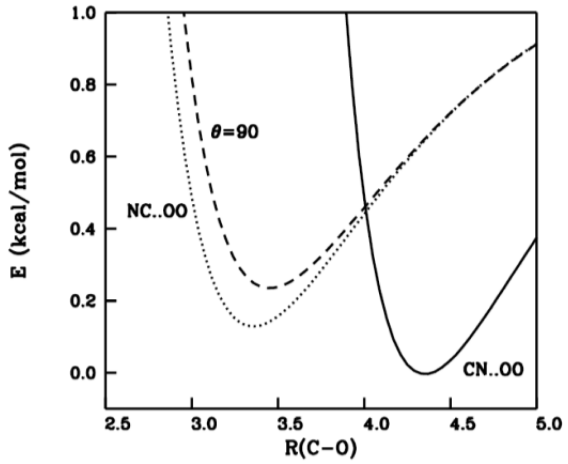


Figure 7. Computed energy profiles for the NC^- and OO system for different orientations of the two bonds. The Θ = 0° is given for $[NC-OO]^-$ configuration. The curves are given as functions of the C···O distances. See main text for additional discussion.

distance at 1.233 Å, while the NCO^- angle is varied. The orientation is such that Θ = 0° corresponds to $[NC-OO]^-$ structure.

We clearly see from the last table and figure that for complexes around the collinear structure the overall thermochemistry is that of an exothermic reaction, while as the O_2 moving gradually around the anionic partner, attacking the NC^- on the N-side, the process becomes increasingly endothermic whenever the O_2 molecule is not dissociating. A pictorial view of this effect is given by the profile of Figure 8. The thermochemical gap is defined as

$V = E_{tot}(NCO^-) + E_{tot}(O) - E_{tot}(CN^-) - E_{tot}(O_2)$, the values given in kcal/mol, and the angle describes once more the linearity at 0° being given by the $[NC-OO]^-$ configuration.

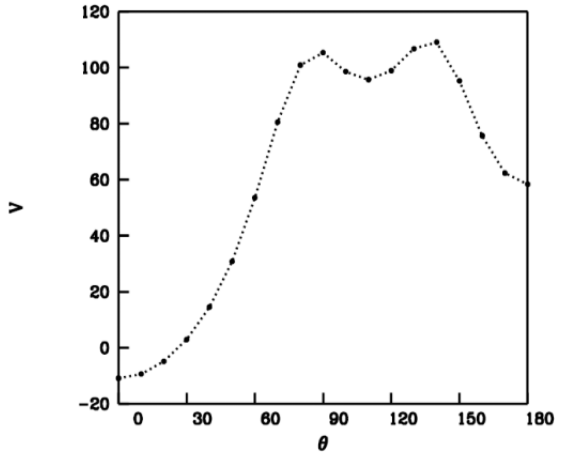


Figure 8. Graphical presentation of the thermochemical energy gap as a function of the NC^-−OO angle, with 0° corresponding to the $[NCO^-+O]$ configuration. See text for a more extensive discussion.

The energy profile reported by Figure 8 confirms the finding of the last table and of the whole previous analysis: the exothermic reaction takes place over a fairly limited angular range for the near-collinear approaches of O_2 on the C-side of the CN^- anionic molecular partner, unless the incoming molecule is also allowed to stretch toward dissociation as it comes closer: NCO^- is stabilized, therefore as O_2 breaks up leaving one oxygen atom as part of the new product anion. Furthermore, the IRC picture of Figure 5 indicates that along such preferred, collinear reaction path the reaction exhibits a marked barrier to its TS configuration.

We can additionally explore the energy landscape of this reaction by the pictorial presentation already used for the radical reaction in Figure 1. This means that we can keep the R_{CN} coordinate constant, define Θ as the angle between NC^- and OO, selecting the Θ = 0° approach to be the more favored $[NCO^-\cdots O]$ structure as in the previous discussion. The results for such reaction path are shown in Figure 9.

Similarly to the case of the radical reaction, we observe that in the products' formation region on the left the TS barrier is displayed (in the lower-left part of the figure) when the oxygen

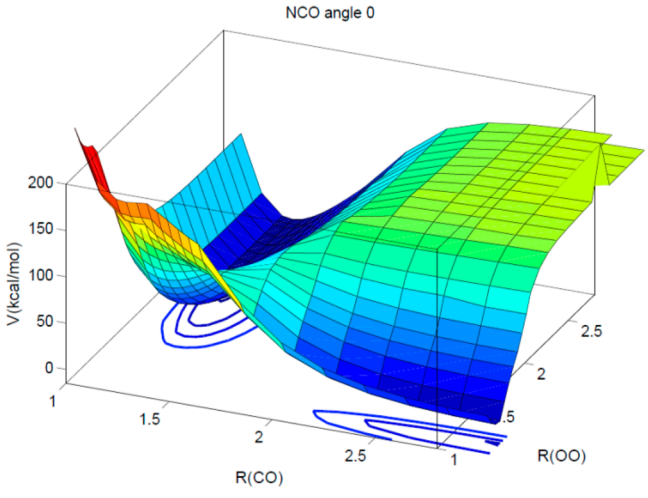


Figure 9. Energy landscape for the ion−molecule reaction with the O_2 partner approaching CN− on the nitrogen end with the R_{CN}^- bond kept fixed at its equilibrium value. See text for further discussion.

Downloaded from pubs.acs.org/jpcafh/article-pdf/120/27/4693/6721384/acs.jpca.5b10472.pdf by KOC UNIV user on 25 October 2026

DOI: 10.1021/acs.jpca.5b10472
J. Phys. Chem. A 2016, 120, 4693−4701

molecule is at its equilibrium geometry (i.e., considered to be a "vibrationally cold" reactive partner). We also see, however;, that the process increasingly becomes more exothermic as the O_2 partner stretches to larger bond distances, to eventually achieve one O atom detachment, although the starting asymptotic energy obviously increases as the O−O vibrational content increases.

Hence, when one starts the reactive process with the R_{OO} coordinate associated with a "vibrationally hot" oxygen molecule at large R_{CO} distances, then the reaction's energy profile uniformly decreases and shows increasingly larger energy gains toward the final products, as the O_2 partner breaks up; no intermediate TS barrier is now visible in the RPES map. Similar effects were also seen and discussed in the case of the radical reaction, which however did not display any barrier to reaction along the collinear approaches.

To better appreciate the angular effects, we repeat in Figure 10, the same data of Figure 9 but this time for two angles of approach (panel a for Θ = 75° and panel b for Θ = 90°) on the N-side of the CN^- partner.

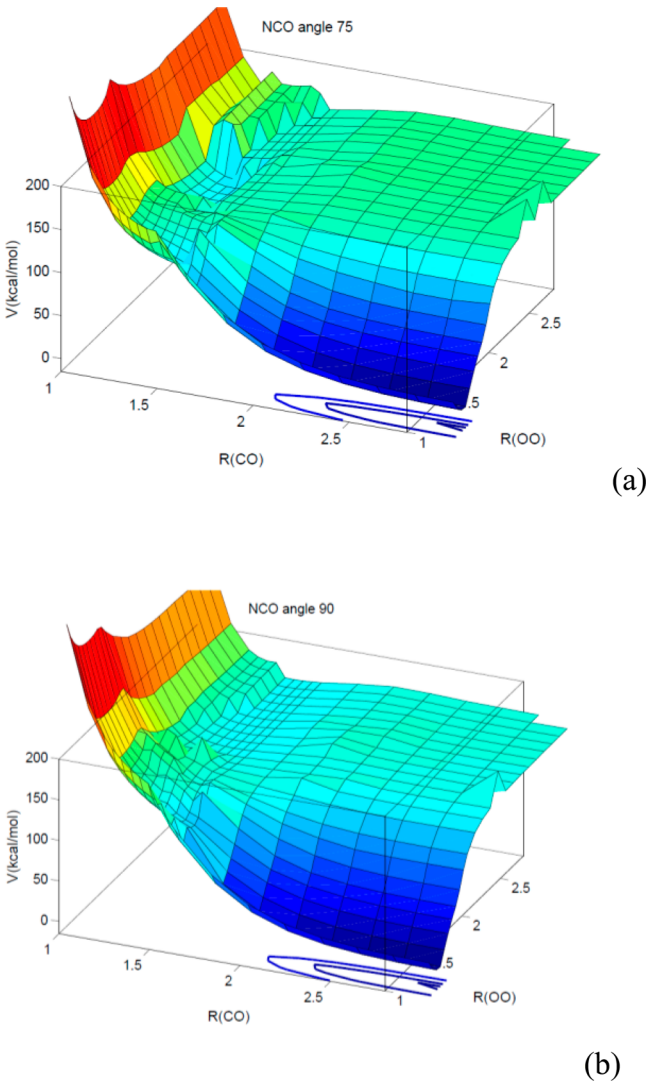


Figure 10. Same graphical presentation as that for the data of Figure 5 but now referring to two bent configurational approaches. See main text for a more extended discussion.

We have already seen that, as the vibrationally cold O_2 molecules gets nearer to the N-end of the CN^- ionic partner, the overall reaction has a clear barrier to products and becomes exothermic as the O−O bond approaches dissociation. Therefore, it can access the NCO^- product with respect to the initial partners when the O_2 molecular bond is already stretched toward O atom detachment. What we see in the two panels of Figure 10 is that the MEP to products is a strongly uphill path when the O_2 is close to its equilibrium geometry and that the reaction becomes mildly exothermic only when that bond is markedly stretched already at the start of the reactive encounters.

The present ion−molecule reaction is thus seen to be exothermic for linear "trajectories" on the C-approach but to exhibit along that path a rather marked barrier to TS formation. It further appears from our study that the stretching of the O−O bond, that is, the presence of "vibrationally hot" molecular oxygen, can make the reaction occur along that path without a barrier to its final products. Both features do not bode well for this chemical path to be an important one at the conditions of the core environments in the DMCs, where one expects that mainly vibrationally cold molecules would be present.

3. PRESENT CONCLUSIONS

It has been proposed[25,26] that the formation of NCO^- could occur through reactions with O_2 molecules. Because accurate calculations and experiments[20] indicated NCO^- to also be its more stable configuration, the search for it in the ISM has been focused on its detection. Furthermore, gas-grain chemical model calculations, representing a wide range of conditions, have been quoted[12] as suggesting that also the neutral radical NCO might be quite abundant in warm sources and also in DMC environments, thus presenting another chemical path for a two-step formation of its anion: the radical reaction with oxygen, as given by eq 4, as a first step provided one further considers REA processes as a second step via the reaction

$$NCO + e^- = >NCO^- + h\nu \quad (6)$$

We have therefore computationally analyzed in detail the energy landscapes for the radical reaction 4, as well as those for the ion−molecule reaction 5 that is directly producing the anionic molecule. Our present calculations, albeit still exploratory in nature, are already able to provide us with the following information:

(i) The oxygen atom detachment from the partner molecule is an important step in controlling the thermochemistry gaps in both reactions. The concurrent stretching of the O−O bond improves in both cases the overall exothermicity of either reaction.

(ii) The collinear path of O_2 approaching on the C-side of either CN or CN^- partners indicate exothermic behavior of the processes as the R_{OO} distance is increased toward dissociation, as the radical or the ionic products are formed, that is, "vibrationally hot" oxygen molecules can help both reactions.

(iii) Only the ionic reaction exhibits the presence of a TS configuration $[NCO^-\cdots O]$ that exists on top of a marked energy barrier. The barrier is most apparent for the collinear approach of reactants and for oxygen molecules remaining close to their initial equilibrium geometry across the whole reaction's.

(iv) On the other hand, the radical reaction is shown to be clearly exothermic for the same collinear approach of reactants and remains so for all other orientational approaches between partners. It further occurs without formation of a TS

Downloaded from pubs.acs.org/jpcafh/article-pdf/120/27/4693/6721384/acs.jpca.5b10472.pdf by KOC UNIV user on 25 October 2026

DOI: 10.1021/acs.jpca.5b10472
J. Phys. Chem. A 2016, 120, 4693−4701

configuration or of a barrier between reactants and products, this being so for all orientations.

One can therefore conclude from the present study, for example, that the direct ion−molecule reaction process would not be very likely to occur under the DMC conditions where low-temperature processes and internally cold reactants are expected to dominate. Because of the relatively light masses of the involved partners, however, the physical possibility for the reagents to tunnel through the barrier in the case of the ion−molecule reaction cannot be excluded, although it would become relevant only in the much higher temperatures of a laboratory, which is an option certainly interesting to pursue in future experiments.

Such findings would thereby make the reaction in eq 5 not to be an energy-convenient chemical path for the NCO^- anion direct formation despite earlier suggestions.[25,26] On the other hand, the radical reaction in eq 4 is shown by the present calculations to be a very attractive option for forming NCO with oxygen molecules because it is a strongly exothermic reaction and it takes place without any barrier or TS configurations when going from reagents to products.

If the NCO neutral molecule would be formed via the above chemical reaction, then the next question is to find whether environmental electrons can play a role in the REA process of eq 1. Several recent studies on electron attachment to polyynes and cyanopolyynes[18,9] have suggested that the efficiency of the REA process for molecular systems with large dipoles ($\mu > 1.6$ D) may occur via the temporary formation of a dipole-type scattering states at threshold energies. This would then favor the direct REA decay into a dipole-type bound state because of the strong spatial similarities between the two extra-electron wave functions.[27] The latter anion could in turn either undergo an internal vibrational redistribution type of mechanism and form a stable valence bound anion or suffer the extra electron loss via autodetachment.

In the present case, the NCO molecule is a polar system but not with a strong dipole (1.5 D), it also has a large electron affinity (3.609 eV),[12] that is, it has to dissipate a fairly large amount of energy on anion stabilization.[28] It is also made up of a small number of atoms: all features suggesting that the indirect electron attachment process would have to involve a large amount of excess energy that has to be dissipated into a fairly small number of available vibrational modes. Because the current modeling of such a process[9,27,28] requires a large number of phase-space mode accessibility for indirect REA process to be efficient, it is difficult to expect the overall REA rates for NCO^- formation at temperatures around those of a cold DMC (i.e., around 20 K or below) to be sufficiently large. As a consequence of the foregoing discussion, the likely formation of NCO ($^3\Sigma^+$) from the reaction with O_2 would not be followed by an efficient second step of stabilization of the negative ion via REA processes with environmental electrons, either directly or indirectly.[18]

In conclusion, the present numerical exploration of possible chemical routes to NCO^- formation via reaction with molecular oxygen suggests that the expected efficiency of such process may not lead to abundances of this anion that were sufficient for it to become observable in molecular clouds. The recent experiments on its search have, in fact, been rather negative[16] and indeed confirm the present findings. Further studies on different routes need to be pursued, as well as more extensive dynamical studies along the paths analyzed in the present work to possibly yield the final reaction rates for both the ion−molecule and the radical mechanisms.

AUTHOR INFORMATION

Corresponding Author

*E-mail: francesco.gianturco@uibk.ac.at. Phone:+39/346-386-9652.

Notes

The authors declare no competing financial interest.

ACKNOWLEDGMENTS

F.A.G. and R.W. thank the FWF, Austrian Science Fund for the Project P27047-N20 for financing this research. E.Y. acknowledges the computational support of the Koç University High Performance Computing Center.

REFERENCES

(1) Watson, W. D. The Rate of Formation of Interstellar Molecules by Ion−Molecule Reactions. *Astrophys. J.* **1973**, *183*, L17−L20.

(2) Herbst, E.; Klemperer, W. Formation and Depletion of Molecules in Dense Interstellat Clouds. *Astrophys. J.* **1973**, *185*, 505−533.

(3) McCall, B. J.; Hinkle, K. A.; Geballe, T. R.; Moriarty-Schieven, G. H.; Evans, N. J., II; Kawaguchi, K.; Takano, S.; Smith, V. V.; Oka, T. Observations of H-3(+) in the Diffuse Interstellar Medium. *Astrophys. J.* **2002**, *567*, 391−406.

(4) Millar, T. J.; Farquhar, P. R. A.; Willacy, K. The UMIST Database for Astrochemistry 1995. *Astron. Astrophys., Suppl. Ser.* **1997**, *121*, 139−185.

(5) Dalgarno, A.; McCray, R. A. Formation of Interstellar Molecules from Negative Ions. *Astrophys. J.* **1973**, *181*, 95−100.

(6) McCarthy, M. C.; Gottlieb, C. A.; Gupta, H.; Thaddeus, P. Laboratory and Astronomical Identification of the Negative Molecular Ion C6H$^-$. *Astrophys. J.* **2006**, *652*, L141−L144.

(7) Cernicharo,J.; Agundez,M.; Guelin,M. Spectral Line Surveys of Evolved Starts. IAO Symposium *280*, 2011, Ed. Cernicharo,J., Bachiller,B., Cambridge University.Press, pg. 237.

(8) Agundez, M.; Cernicharo, J.; Guelin, M.; Kahane, C.; Roueff, E.; Klos, J.; Aoiz, F.; Lique, F.; Marcelino, N.; Goicochea, J. R. Astronomical Identification of CN^-, the Smallest Observed Molecular Anion. *Astron. Astrophys.* **2010**, *517*, L2.

(9) Satta, M.; Gianturco, F. A.; Carelli, F.; Wester, R. A Quantum Study of the Chemical Formation of CYANO ANIONS in Inner Cores and Diffuse Regions of Interstellar Molecular Clouds. *Ap.J.* **2015**, *799*, 228.

(10) Bradforth, S. E.; Kim, E. H.; Arnold, D. W.; Newmark, D. M. Photoelectron-Spectroscopy of CN^-, NCO^-, and NCS^-. *J. Chem. Phys.* **1993**, *98*, 800−810.

(11) Pak, Y.; Woods, R. C.; Peterson, K. A. Coupled Cluster Spectroscopic Properties and Isomerization Pathway for the Cyanate/Fulminate Isomer Pair, NCO^-/CNO^-. *J. Chem. Phys.* **1997**, *106*, 5123−5132.

(12) Lattanzi, V.; Gottlieb, C. A.; Thaddeus, P.; McCarthy, M. C. The Rotational Spectrum of the NCO^- Anion. *Astrophys. J.* **2010**, *720*, 1717−1720.

(13) Schutte, W. A.; Greenberg, J. M. Further Evidence for the OCN^- Assignment to the XCN Band in Astrophysical Ice Analogs. *Astron. Astrophys.* **1997**, *317*, L43−L46.

(14) Ehrenfreund, P.; Charnley, S. B. Organic Molecules in the Interstellar Medium, Comets, and Meteorites: A Voyage from Dark Clouds to the Early Earth. *Annu. Rev. Astron. Astrophys.* **2000**, *38*, 427−483.

(15) van Broekhuizen, F. A.; Keane, J. V.; Schutte, W. A. A Quantitative Analysis of OCN^- Formation in Interstellar Ice Analogs. *Astron. Astrophys.* **2004**, *415*, 425−436.

(16) Morisawa, Y.; Hoshina, H.; Kato, Y.; Simizo, Z.; Kuma, S.; Sogoshi, N.; Fushitami, M.; Watanabe, S.; Miyamoto, Y.; Momose, T.;

DOI: 10.1021/acs.jpca.5b10472
J. Phys. Chem. A 2016, 120, 4693−4701

Downloaded from pubs.acs.org/jpcafh/article-pdf/120/27/4693/6721384/acs.jpca.5b10472.pdf by KOC UNIV user on 25 October 2026

Kasai, Y.; Kanagachi, K. Search for CCH^-, NCO^-, and NCS- Negative Ions in Molecular Clouds. *Publ. Astron. Soc. Jpn.* **2005**, *57*, 325−334.
(17) Kaur, S.; Baluja, K. L. Electron-Impact Study of an NCO Molecule Using the R-Matrix Method. *Phys. Rev. A: At., Mol., Opt. Phys.* **2012**, *85*, 052701.
(18) Douguet, N.; Fonseca dos Santos, S.; Raoult, M.; Dulieu, O.; Orel, A.; Kokuline, V. Theory of Radiative Electron Attachment to Molecules: Benchmark study of CN^-. *Phys. Rev. A: At., Mol., Opt. Phys.* **2013**, *88*, 052710.
(19) Frisch, M. J.; Trucks, G. W.; Schlegel, H. B.; Scuseria, G. E.; Robb, M. A.; Cheeseman, J. R.; Scalmani, G.; Barone, V.; Mennucci, B.; Petersson, G. A.; et al. *Gaussian 09*, revision D.01; Gaussian Inc.: Wallingford, CT, 2013.
(20) Leonard, C.; Gritli, H.; Chambaud, G. New Study of the Stability and of the Spectroscopy of the Molecular Anions NCO^- and CNO^-. *J. Chem. Phys.* **2010**, *133*, 124318.
(21) Werner, H.-J.; Knowles, P. J. A 2nd Order Multiconfiguration SCF Procedure with Optimum Convergence. *J. Chem. Phys.* **1985**, *82*, 5053−5063.
(22) Knowles, P. J.; Werner, H.-J An Efficient Method for the Evaluation of Coupling_Coefficients in Configuration-Interaction Calculations. *Chem. Phys. Lett.* **1988**, *145*, 514−522.
(23) Fukui, K. A Formulation of Reaction Coordinate. *J. Phys. Chem.* **1970**, *74*, 4161.
(24) Crehuet, R.; Bofill, J. M. The Reaction Path Intrinsic Reaction Coordinate Method and the Hamilton-Jacobi Theory. *J. Chem. Phys.* **2005**, *122*, 234105.
(25) Iglesias, E. Chemical Evolution of Molecular Clouds. *Astrophys. J.* **1977**, *218*, 697−715.
(26) Prasad, S. S.; Huntress, W. T., Jr. NCO^- Potential Inter-Stellar Species. *Mon. Not. R. Astron. Soc.* **1978**, *185*, 741−744.
(27) Carelli, F.; Satta, M.; Grassi, T.; Gianturco, F. A. Carbon-Rich Molecular Chains in Protoplanetary and Planetary Atmospheres: Quantum Mechanisms amd Electron Attachment Rates for Anion Formation. *Astrophys. J.* **2013**, *774*, 97.
(28) Petrie, S.; Herbst, E. Some Interstellar Reactions Involving Electrons and Neutral Species: Attachment and Isomerization. *Astrophys. J.* **1997**, *491*, 210−215.

Downloaded from pubs.acs.org/jpcafh/article-pdf/120/27/4693/6721384/acs.jpca.5b10472.pdf by KOC UNIV user on 25 October 2026

DOI: 10.1021/acs.jpca.5b10472
J. Phys. Chem. A 2016, 120, 4693−4701